Published August 27, 2001

JCB Article

An effector region in Eps8 is responsible for the activation of the Rac-specific GEF activity of Sos-1 and for the proper localization of the Rac-based actin–polymerizing machine

Giorgio Scita,[1] Pierluigi Tenca,[1] Liliana B. Areces,[1] Arianna Tocchetti,[1] Emanuela Frittoli,[1] Giuseppina Giardina,[1] Isabella Ponzanelli,[1] Patrizia Sini,[1] Metello Innocenti,[1] and Pier Paolo Di Fiore[1,2,3]

[1]Department of Experimental Oncology, European Institute of Oncology, 20141 Milan, Italy
[2]The Firc Institute for Molecular Oncology, 20134 Milan, Italy
[3]Department of Medicine, Surgery, and Odontoiatry, University of Milan, 20122 Milan, Italy

Genetic and biochemical evidence demonstrated that Eps8 is involved in the routing of signals from Ras to Rac. This is achieved through the formation of a tricomplex consisting of Eps8–E3b1–Sos-1, which is endowed with Rac guanine nucleotide exchange activity. The catalytic subunit of this complex is represented by Sos-1, a bifunctional molecule capable of catalyzing guanine nucleotide exchange on Ras and Rac. The mechanism by which Sos-1 activity is specifically directed toward Rac remains to be established. Here, by performing a structure–function analysis we show that the Eps8 output function resides in an effector region located within its COOH terminus. This effector region, when separated from the holoprotein, activates Rac and acts as a potent inducer of actin polymerization. In addition, it binds to Sos-1 and is able to induce Rac-specific, Sos-1–dependent guanine nucleotide exchange activity. Finally, the Eps8 effector region mediates a direct interaction of Eps8 with F-actin, dictating Eps8 cellular localization. We propose a model whereby the engagement of Eps8 in a tricomplex with E3b1 and Sos-1 facilitates the interaction of Eps8 with Sos-1 and the consequent activation of an Sos-1 Rac–specific catalytic ability. In this complex, determinants of Eps8 are responsible for the proper localization of the Rac-activating machine to sites of actin remodeling.

Introduction

Small GTPases function as critical relays in the transduction of signals originating from membrane receptors by cycling between inactive GDP– and active GTP–bound states. Guanine nucleotide exchange factors (GEFs)* catalyze the exchange of GDP for GTP, thus controlling the rate and timing of activation of small GTPases. The activation of receptor tyrosine kinases (RTKs), resulting in the reorganization of the actin cytoskeleton, is one of the best characterized pathways controlled by these molecular switches. Active ligand–engaged RTKs signal to a critical small GTPase, Ras, which in turn activates another small GTPase, Rac. Finally, active GTP–bound Rac is directly responsible for molecular events leading to actin remodeling (for review see Bar-Sagi and Hall, 2000; Scita et al., 2000).

The molecular mechanisms of this cascade are being elucidated. Biochemical and genetic studies have shown how the Son of Sevenless (Sos)-1 GEF transduces the signal from active RTKs to Ras (for review see Bar-Sagi, 1994; Schlessinger, 2000). Sos-1 interacts with the SH3-containing adaptor molecule Grb2. Grb2 in turn displays an SH2 domain responsible for the recruitment of the Grb2–Sos-1 complex to active, autophosphorylated RTKs. The relocalization of the complex to the plasma membrane is thought to be sufficient for Sos-1 to catalyze the exchange of guanine

The online version of this article contains supplemental material.

Address correspondence to Pier Paolo Di Fiore, Department of Experimental Oncology, European Institute of Oncology, Via Ripamonti, 435, 20141 Milano, Italy. Tel.: (39) 025-748-9833. Fax: (39) 025-748-9851. E-mail: pdifiore@ieo.it

G. Scita and P. Tenca contributed equally to this work.

*Abbreviations used in this paper: Ab, antibody; GEF, guanine nucleotide exchange factor; GFP, green fluorescent protein; MAPK, mitogen-activated protein kinase; MBP, myelin basic protein; PIP3, phosphatidylinositol 3,4,5 trisphosphate; PI3-K, phosphatidylinositol 3 kinase; RTK, receptor tyrosine kinase; Sos, Son of Sevenless.

Key words: Eps8; Rac; Sos-1; cytoskeleton; GEF

Supplemental Material can be found at:
http://jcb.rupress.org/content/suppl/2001/08/24/jcb.200103146.DC1.html

Published August 27, 2001

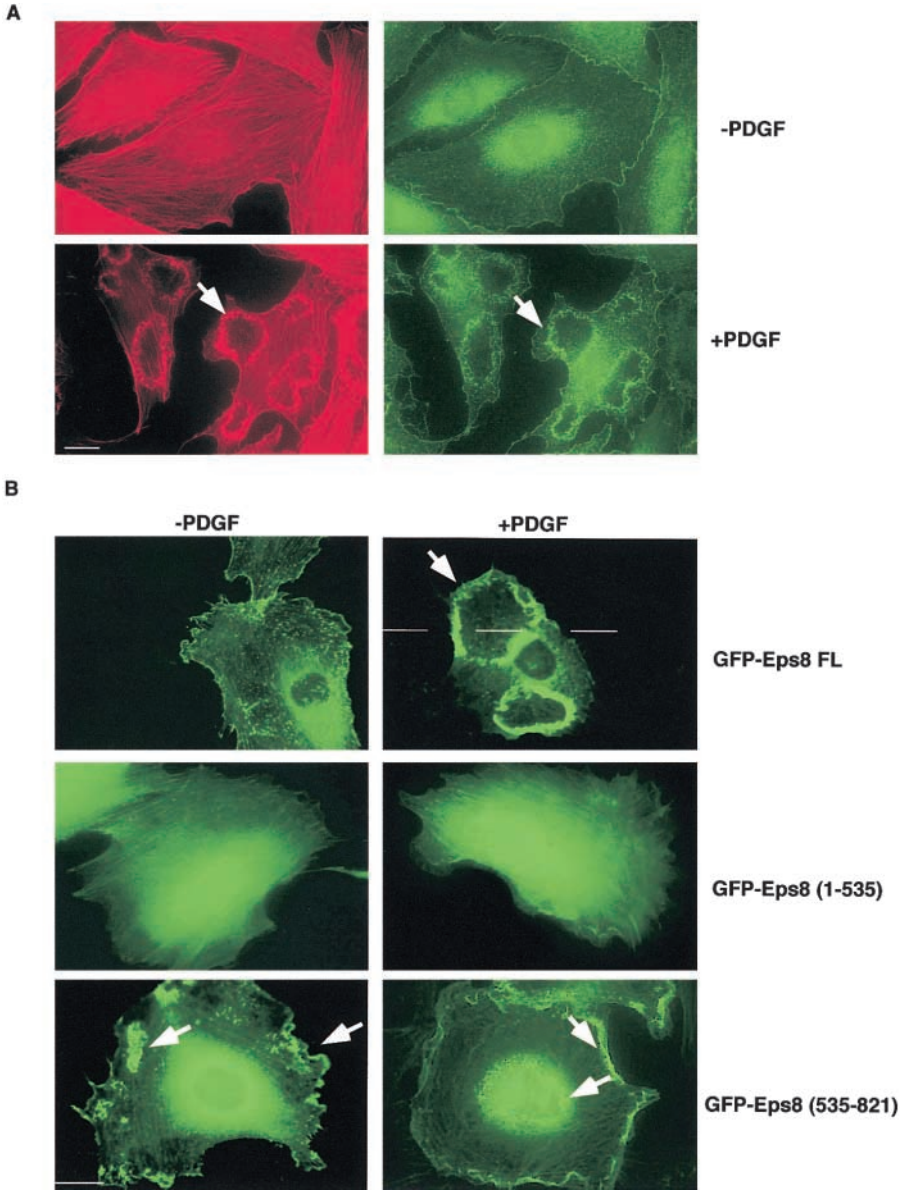

Figure 1. **The COOH-terminal region (535–821) of Eps8 is necessary and sufficient for Eps8 localization to the cell cortex and its accumulation into PDGF-induced membrane ruffles.** (A) Mouse embryo fibroblasts were serum starved for 24 h and then treated with 10 ng/ml of PDGF (+PDGF) for 10 min or mock treated (−PDGF). Fibroblasts were fixed and stained with rhodamine-conjugated phalloidin (red, left) to detect F-actin or anti-Eps8 (green, right). Ruffling was detected in >90% of the PDGF-treated cells. (B) Mouse embryo fibroblasts were transfected with expression vectors encoding Eps8 full length or the indicated Eps8 fragments fused to GFP (FL, full length; amino acid boundaries of the other constructs are given in parentheses). After serum starvation, cells were treated with 10 ng/ml of PDGF (+PDGF) for 10 min or mock treated (−PDGF), followed by fixation and detection of GFP-Eps8 fusion proteins by epifluorescence. Representative pictures are shown. In B, ruffles were identified by costaining with phalloidin (not shown). Arrowheads point to ruffles. Bars, 10 μm.

nucleotides on Ras, which is also present at the plasma membrane.

How Ras signals to Rac is less understood. Phosphatidylinositol 3 kinase (PI3-K) binds directly to Ras-GTP and it is required for activation of Rac (for review see Rodriguez-Viciana et al., 1997). In hematopoietic cells, the product of PI3-K's catalytic activity, phosphatidylinositol 3,4,5 trisphosphate (PIP3), contributes through direct binding to the activation of a Rac-specific GEF, Vav-1 (Han et al., 1998; Das et al., 2000). In nonhematopoietic cells, the lack of expression of Vav-1 indicates that other GEFs must be involved. Indeed, two recently identified members of the Vav family, Vav2 and Vav3, display ubiquitous expression and have been implicated in RTK-mediated actin remodelling (Schuebel et al., 1998; Liu and Burridge, 2000; Moores et al., 2000; Trenkle et al., 2000).

Sos-1 was also implicated in Ras-to-Rac signaling (Nimnual et al., 1998; Scita et al., 1999). Sos-1 was shown to participate in vivo in a tricomplex with two signaling molecules, Eps8 (Fazioli et al., 1993) and E3b1 (also known as Abi-1) (Shi et al., 1995; Biesova et al., 1997). E3b1 contains an SH3 domain that mediates its binding to Sos-1 (Scita et al., 1999; Fan and Goff, 2000). In addition, E3b1 binds to the SH3 domain of Eps8, thus acting as a scaffold protein which holds together Sos-1 and Eps8 (Biesova et al., 1997; Mongiovi et al., 1999; Scita et al., 1999). The tricomplex Sos-1–E3b1–Eps8 displays Rac GEF activity in vitro (Scita et al., 1999). Therefore, Sos-1 might be endowed with a dual GEF activity, for Ras and Rac, respectively. At the molecular level, this is mirrored by the presence of two GEF domains in Sos-1: (a) a Cdc25-like domain, responsible for activity on Ras, and (b) a DH-PH tandem domain, a hallmark of GEFs for Rho GTPases, the subfamily to which Rac belongs. However, purified Sos-1 does not display Rac-GEF activity, whereas Ras-GEF activity could be readily detected. Thus, a coherent picture of how Sos-1 regulates Rac activation is still missing. Another unresolved question concerns the mechanism responsible for the proper compartmentalization of Sos-1 to sites where the Rac-based actin polymerizing machinery needs to be active. In this study, we provide

Published August 27, 2001

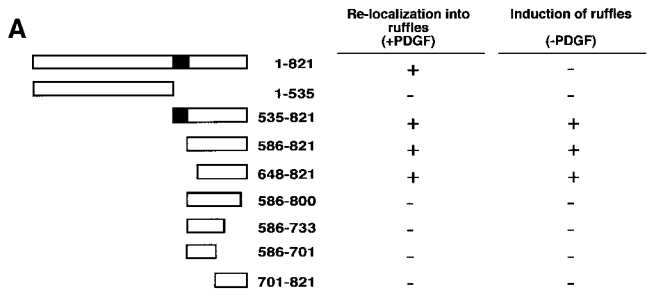

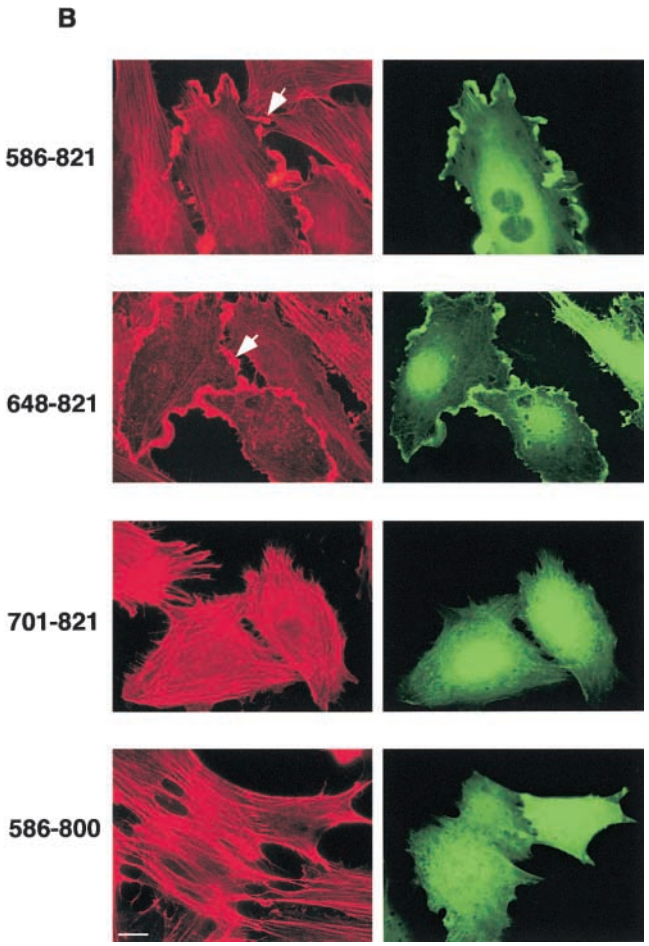

Figure 2. **Identification of the minimal effector region of Eps8 capable of inducing actin polymerization into ruffles.** (A) Schematic of the various Eps8 fragments, all engineered as GFP fusion proteins (amino acid boundaries are given on the left of the constructs. The SH3 domain is indicated by a solid box), and their biological characterization. Mouse embryo fibroblasts, transfected with the indicated GFP-tagged expression vectors, were serum starved and treated with 10 ng/ml of PDGF for 10 min (+PDGF) or mock treated (−PDGF). Cells were then fixed for subsequent detection of GFP by epifluorescence and F-actin by rhodamine-conjugated phalloidin. (B) Mouse embryo fibroblasts, transfected with the indicated expression vectors, were serum-starved and fixed for subsequent detection of GFP by epifluorescence (green), and F-actin by rhodamine-conjugated phalloidin (red). Actin polymerization into ruffles induced by the biologically active Eps8 fragments was detected in >80% of the transfected cells. The effect of selected constructs is shown. Arrows point to ruffles. Bar, 10 μm.

evidence that Eps8 is a critical factor in the regulation of both these functions.

Results

Identification of a COOH-terminal "effector region" of Eps8 capable of inducing actin polymerization into ruffles

The biochemical function of Eps8, which mediates Ras to Rac signaling, leading to actin cytoskeleton reorganization (Scita et al., 1999, 2000), is mirrored by its subcellular localization. In serum-starved fibroblasts, Eps8 displays a punctuate, cytoplasmic perinuclear distribution with some staining at the plasma membrane corresponding to sites of cortical actin accumulation (Provenzano et al., 1998; Scita et al., 1999; Fig. 1 A). A substantial relocalization of Eps8 occurs upon treatment with growth factors within sites of actin polymerization, at the dorsal surface of cells, and in membrane ruffles (Provenzano et al., 1998; Scita et al., 1999; Fig. 1 A).

To identify the region of Eps8 that mediates its localization, we used deletion mutants of Eps8 fused to the green fluorescence protein (GFP). A GFP full length Eps8 (amino acids 1–821) displayed a sub-cellular localization indistinguishable from that of the endogenous protein (Fig. 1 B). In contrast, a NH_2-terminal fragment (amino acids 1–535) showed a diffuse cytoplasmic and nuclear staining unaltered by treatment with growth factors, suggesting that the COOH terminus contains residues important for Eps8 localization (Fig. 1 B). Accordingly, a COOH-terminal fragment (amino acids 535–821) displayed intense localization along the cell cortex within structures reminiscent of ruffles. These structures corresponded to sites of actin polymerization (not shown; see also Fig. 2). The differential cellular localization of the Eps8 mutants was not due to the GFP moiety, since GFP alone was diffusely distributed in the nucleus and the cytoplasm (not shown). Furthermore, similar levels of expression of the various Eps8 constructs were obtained, as determined by immunoblotting (not shown) and immunofluorescence analysis (Fig. 1 B). Thus, our data indicate that determinants in the COOH terminus are responsible for the subcellular localization of Eps8.

An unexpected finding emerged from the studies with the Eps8 (535–821) mutant. In serum-starved mouse embryo fibroblasts, where the actin cytoskeleton is organized in a flat array of stress fibers, the expression of this mutant caused reorganization of F-actin into dorsal and membrane ruffles (Fig. 2 B). This effect could also be observed in different cell lines (Cos-7, NIH-3T3, HeLa; not shown). Thus, the COOH terminus of Eps8 is responsible not only for proper localization of the protein, but it also displays an "effector" function, capable of inducing actin cytoskeleton remodeling in the absence of growth factor stimulation.

Mapping of the effector region of Eps8

We engineered a series of deletion mutants of Eps8 (Fig. 2 A) fused to GFP. A mutant, 586–821, lacking the SH3 do-

Published August 27, 2001

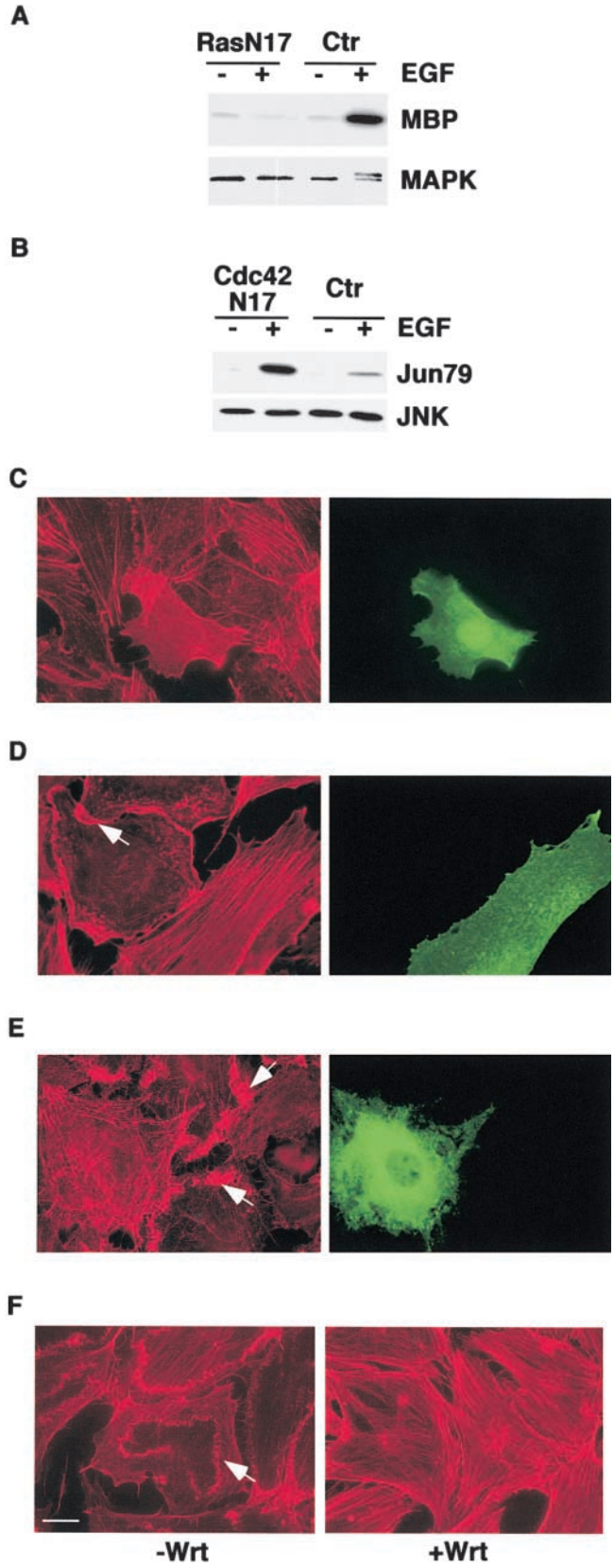

Figure 3. **Expression and biological activity of dominant negative mutants of Ras, Cdc42, Rho, Rac, PI-3K, and of the PI-3K inhibitor, wortmannin.** (A) Mouse embryo fibroblasts were cotransfected with an expression vector encoding RasN17 (Ras N17) or an empty vector as a control (Ctr), together with pCDNA-HA-MAPK. Cells were serum starved for 24 h and treated with 100 ng/ml of EGF (+) or mock treated (−) for 10 min. MAPK kinase activity was determined in immunocomplex kinase assays using myelin basic protein (MBP) as a substrate. An aliquot of the immunoprecipitates was also immunoblotted with anti-MAPK antibodies (MAPK). The doublet MAPK band, detected in the EGF-treated control sample, represents the active phosphorylated form. (B) Mouse embryo fibroblasts were cotransfected with expression vectors encoding a dominant negative HA-tagged Cdc42 (Cdc42N17) or an empty vector as a control (Ctr) together with pCDNA-HA-JNK, serum starved for 24 h, and treated with 100 ng/ml of EGF (+) or mock treated for 10 min (−). JNK kinase activity was determined in immunocomplex kinase assays, using the COOH-terminal region of c-JUN (Jun79) as a substrate. An aliquot of the immunoprecipitates was also immunoblotted with anti-JNK antibodies (JNK). The expression of RasN17 in A and HA-Cdc42N17 in B was determined by immunoblot analysis with anti-Ras and anti-HA antibodies, respectively (not shown). (C–E). Nuclei of quiescent mouse embryo fibroblasts were microinjected with expression vectors encoding RhoN19 (C), RacN17 (D), or p85ΔiSH2 (E). After 3 h, cells were stimulated with either 10% serum for 60 min (C) or PDGF (10 ng/ml) for 10 min (D and E) and fixed and stained with rhodamine-conjugated phalloidin (red) to detect F-actin, anti-Rho (C, green), anti-Rac (D, green) or anti-p85 (E, green) antibodies. (F) Quiescent mouse embryo fibroblasts were treated with wortmannin (100 nM) (+Wrt) or vehicle as a control (−Wrt) for 1 h before adding PDGF for 10 min. Cells were then fixed and stained with phalloidin (red). Arrows point to ruffles. Bar, 10 μm.

main retained ruffling activity in the absence of growth factor treatment (Fig. 2, A and B), indicating that the SH3 domain of Eps8 is dispensable for actin reorganization activity in the absence of growth factors. Thus, an interaction with E3b1, mediated by the SH3 domain of Eps8, is not required for the effector function of the COOH-terminal fragment of Eps8.

Further deletions of the COOH terminus of Eps8 (Fig. 2, A and B) showed that the minimal region required to elicit ruffling spanned amino acids 648–821. Interestingly, this region is also the minimal region required for colocalization with polymerized actin (Fig. 2 A). Indeed, for all the Eps8 mutants containing this region, there was perfect correlation between ruffling activity and colocalization with phalloidin-stained F-actin (or lack of both events; Fig. 2 A). Notably, the Eps8 effector region, similarly to the known inducer of actin polymerization such as activated Rac and PI3-K, induces prominent peripheral ruffles, but only rarely circular ruffles. These latter structures are dependent on PDGF stimulation, pointing to the requirement of additional signaling events, whose nature remains undetermined.

The ruffle-inducing activity of the Eps8 effector region was recorded in real time. The GFP effector region of Eps8 (586–821) rapidly induced and accumulated within dynamic structures along the dorsal area and the leading edge of cells, thus confirming the observations obtained in paraformaldehyde-fixed cells. Furthermore, it relocalized in protruding lamellipodia of spreading and moving cells, suggesting its involvement in migratory processes (supplementary information). Thus, Eps8 is endowed with a potent and constitutive ruffle-inducing activity residing in its 173 COOH-terminal amino acids.

Signaling by the effector region of Eps8

Ras and Rho GTPases establish a signaling network that regulates actin rearrangement (for review see Bar-Sagi and Hall, 2000; Scita et al., 2000), a process in which the participation of PI3-K has also been firmly established (for review see

Published August 27, 2001

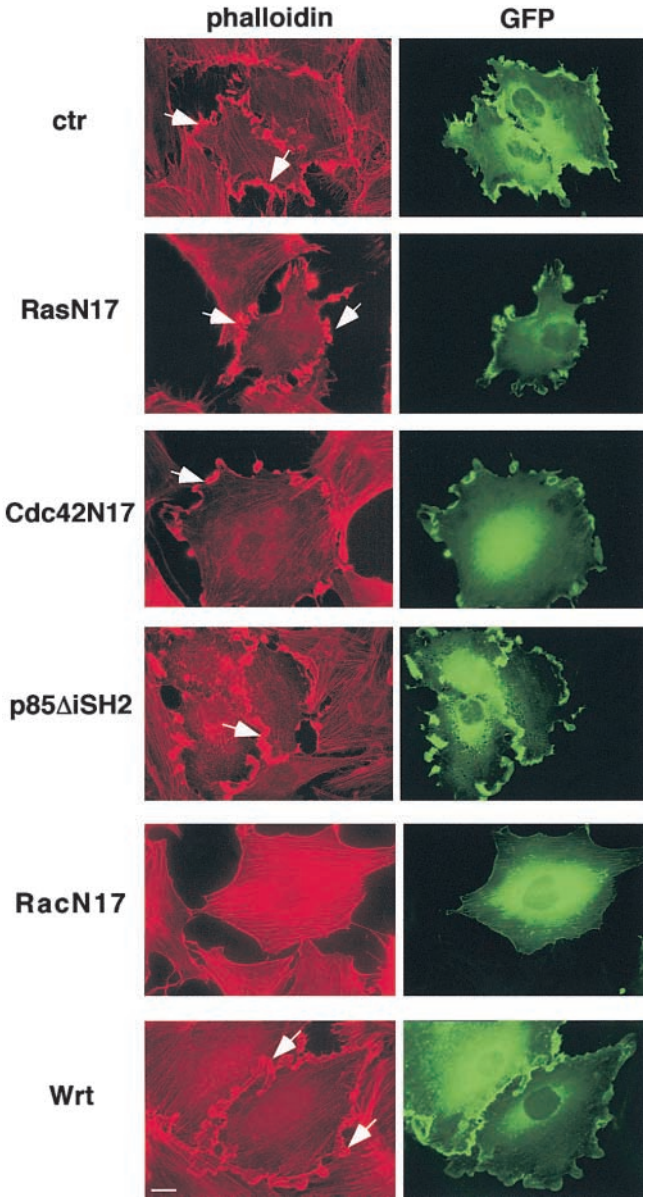

Figure 4. **The effector region of Eps8 requires Rac for its actin remodelling activity.** Nuclei of quiescent mouse embryo fibroblasts were comicroinjected with the expression vector for GFP-Eps8 (648–821) (all panels) together with one of the indicated (left) dominant negative mutants (ctr, comicroinjection with control vector). In the bottom panels (Wrt), microinjection was with GFP-Eps8 (648–821) alone followed by treatment with wortmannin for 60 min. After 3 h, cells were fixed and detection of GFP was performed by epifluorescence (green), whereas F-actin was detected by phalloidin staining (red). All the comicroinjected cells expressed the GFP-Eps8 (648–821) fragment and the individual dominant negative mutant, as determined in parallel experiments, by directly staining the microinjected cells with antibodies specific to the various dominant negative mutants (not shown). More than 100 injected cells were analyzed in each experiment. Similar results were obtained in transfection experiments. Arrows point to ruffles. Bar, 10 μm.

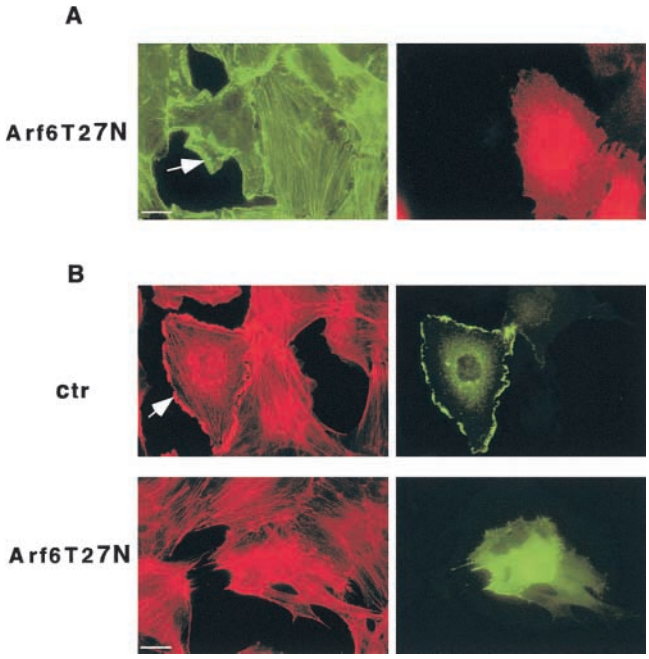

Figure 5. **A dominant negative Arf6 mutant inhibits ruffling induced by GFP-Eps8 (648–821).** (A) Nuclei of quiescent mouse embryo fibroblasts were microinjected with the expression vector encoding a dominant negative Arf6 (Arf6T27N). After 3 h cells were stimulated with PDGF (10 ng/ml) for 10 min, and then fixed and stained with FITC-conjugated phalloidin (green) to detect F-actin and with the anti-myc antibody to detect Arf6T27N (red). Arf6T27N inhibited PDGF-induced ruffling in 90 ± 4% (mean ± SE) of the injected cells, as compared with cells injected with an empty vector. (B) Nuclei of quiescent mouse embryo fibroblasts were microinjected with expression vectors for GFP-Eps8 (648–821) (all panels) together with either a control vector (ctr) or a vector encoding myc-Arf6T27N (Arf6T27N). After 3 h, cells were fixed and detection of GFP was performed by epifluorescence (green). Phalloidin (red) staining was also performed. All the comicroinjected cells expressed both the GFP-Eps8 (648–821) fragment and the Arf6T27N mutant, as determined in parallel experiments by directly staining the microinjected cells with anti-myc antibodies to detect Arf6T27N (not shown). More than 100 injected cells were analyzed in each experiment. Similar results were obtained in transfection experiments. Arrows point to ruffles. Bars, 10 μm.

Rodriguez-Viciana et al., 1997). To define the site of action of the effector region of Eps8 in the signaling pathways leading to actin remodeling, we attempted to interfere with its function with a series of molecular and pharmacological inhibitors. In particular, we used dominant negative versions of Ras (RasN17), Cdc42 (Cdc42N17), Rho (RhoN19), PI3-K (p85ΔiSH2), and Rac (586-821). We also used the PI3-K–specific inhibitor, wortmannin.

Upon microinjection in mouse fibroblasts, all the dominant negative mutants were readily expressed (Fig. 3) and biologically active, as shown by the ability of: (a) RasN17 to inhibit EGF-induced mitogen-activated protein kinase (MAPK) activation (Fig. 3 A); (b) Cdc42N17 to reduce growth factor–induced JNK activity (Fig. 3 B); (c) RhoN19 to inhibit the formation of serum-induced stress fibers (Fig. 3 C); and (d) RacN17 (Fig. 3 D) and p85ΔiSH2 (Fig. 3 E) to inhibit PDGF-mediated actin cytoskeleton reorganization. Wortmannin also abrogated completely PDGF-induced actin remodeling (Fig. 3 F).

We then attempted to interfere with the ruffling activity of GFP-Eps8 (648–821) by comicroinjecting the dominant negative mutants or by treating cells microinjected with this latter construct with wortmannin. Ruffling activity was unaffected by coexpression of dominant negative Ras, Cdc42, Rho, or PI3-K, or by treatment with wortmannin (Fig. 4).

Published August 27, 2001

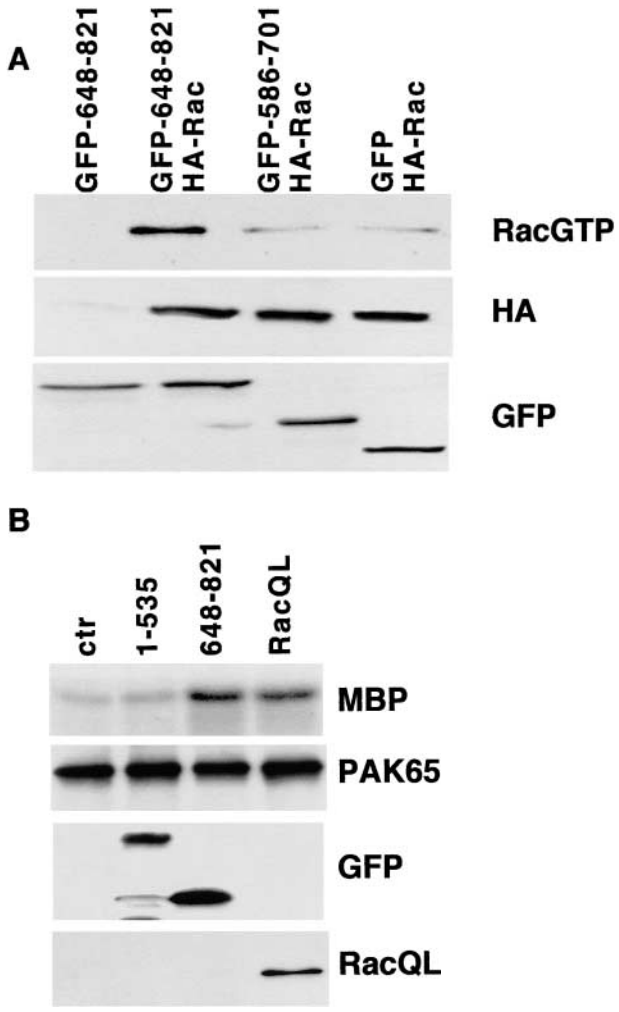

Figure 6. **The effector region of Eps8 activates Rac and Rac-dependent biochemical pathways.** (A) The expression vectors indicated on the top, and encoding GFP-Eps8 (648–821), GFP-Eps8 (586–701), GFP, and HA-Rac were transfected, alone or in combination, into mouse embryo fibroblasts. After 24 h of serum deprivation, Rac-GTP levels were determined by an in vitro binding assay using the CRIB domain of PAK65 fused to GST (top). Aliquots of the lysates were also analyzed for the expression of the GFP or the GFP-tagged Eps8 fragments and of HA-Rac by direct immunoblot (bottom). (B) Mouse embryo fibroblasts were cotransfected with expression vectors for HA-PAK65 together with the indicated (top) GFP-tagged Eps8 fragments (1–535 or 648–821), an activated Rac mutant (RacQL), or an empty vector as a control (ctr). After 24 h of serum deprivation, PAK65 kinase activity was determined by immunocomplex kinase assays using MBP as a substrate (MBP). An aliquot of the immunoprecipitates used for each kinase assay was immunoblotted with anti-HA to detect PAK65 (PAK65). Aliquots of the lysates were also analyzed for the expression of the GFP-tagged Eps8 fragments and of RacQL by direct immunoblot (GFP and RacQL).

However, the expression of a dominant negative Rac abrogated the GFP-Eps8 (648–821)–induced ruffles (Fig. 4). Thus, the ruffling activity of the effector region of Eps8 is apparently exerted at a step upstream of Rac and does not require the functions of Ras and PI3-K.

The dependence on Rac activity of the effect of GFP-Eps8 (648–821) was further supported by experiments performed with a dominant negative Arf6 mutant. Arf6 is a protein belonging to the Arf subfamily of small GTPases (Donaldson and Radhakrishna, 2001). A dominant negative Arf6 blocks Rac-dependent actin reorganization, likely by preventing the translocation of GTP-bound Rac from an endosomal compartment to the plasma membrane (Radhakrishna et al., 1999; Zhang et al., 1999; Fig. 5 A). Microinjection, in mouse fibroblasts, of a dominant negative mutant Arf6 (Arf6T27N) capable of abrogating Rac-dependent PDGF-induced ruffles inhibited GFP-Eps8 (648–821)–dependent actin cytoskeleton rearrangement (Fig. 5 B), compatible with the requirement for proper localization of Rac.

The effector region of Eps8 activates Rac and Rac-dependent pathways, binds to Sos-1, and stimulates Rac-specific, Sos-1–dependent GEF activity

The Rac-dependent ruffling activity of the effector region of Eps8 suggests that it may act by activating Rac. Thus, we tested the ability of the 648–821 region of Eps8 to induce the activation of Rac and of PAK65, a direct downstream effector of Rac (for review see Lim et al., 1996). As shown in Fig. 6 A, the expression in quiescent fibroblasts of GFP-Eps8 (648–821), but not of GFP or GFP-Eps8 (586–701), increased the levels of activated GTP-bound Rac. This was mirrored by the activation of PAK65 to levels similar to those induced by a constitutively active Rac mutant. These results indicate that the effector region of Eps8 activates Rac in vivo.

Therefore, the effector region of Eps8 seems to recapitulate the physiological function of Eps8, behaving as a dominant active mutant and bypassing the need for growth factor stimulation. However, at variance with Eps8, the effector region does not require a physical interaction with E3b1 (Figs. 2, and 7, A and C) and the ensuing formation of a trimeric complex with Sos-1. On the other hand, the COOH terminus of Eps8 has been shown to bind in vitro to Sos-1 independently of E3b1 (Scita et al., 1999), albeit with low stoichiometry. Thus, this interaction may be sufficient to elicit Sos-1 guanine nucleotide exchange activity, leading to the activation of Rac in vivo.

To test this possibility, we first mapped the region of Eps8 that binds to Sos-1. Native Sos-1 could be specifically recovered onto GST-fused Eps8 COOH-terminal frag-

Figure 7. **The Eps8 effector region binds to Sos-1 and stimulates Rac-specific, Sos-1–dependent GEF activity.** (A) Total cellular lysates from Cos-7 cells were incubated with 5 μg of each Eps8 fragment (all engineered as GST fusions; amino acid boundaries are indicated at the top) or GST as a negative control, or GST-E3b1 as a positive control (Scita et al., 1999). Detection was with anti–Sos-1 Ab. The lane "lysate" was loaded with 50 μg of total cellular lysate. (B) Left, eukaryotically produced, affinity-purified Sos-1 was resolved by SDS-PAGE and stained with Coomassie brilliant blue. Sos-1 was estimated to be >90% pure (see Materials and methods). Right, purified Sos-1 (1 μg) was incubated with 5 μg of the indicated GST fusion proteins (all Eps8 fragments; amino acids boundaries are indicated on the top). Detection was with anti–Sos-1 Ab. The binding of Sos-1 to full length Eps8 (1–821) was estimated to be ~10 less than the binding to GST-Eps8 (586–821) or GST-Eps8 (648–821) by densitometric analysis. (C) Lysates of 293T cells transfected with the indicated cDNAs (tfx) were immunoprecipitated (IP) with anti-Eps8 (Eps8) or anti-HA (HA), or the corresponding preimmune sera (ctr) followed by detection (Western blot, WB) with anti–Sos-1, anti-Eps8, anti-E3b1, or anti-HA antibodies. Native Sos-1 could also be recovered in immunoprecipitates of the Eps8 fragments 648–821 (not

Published August 27, 2001

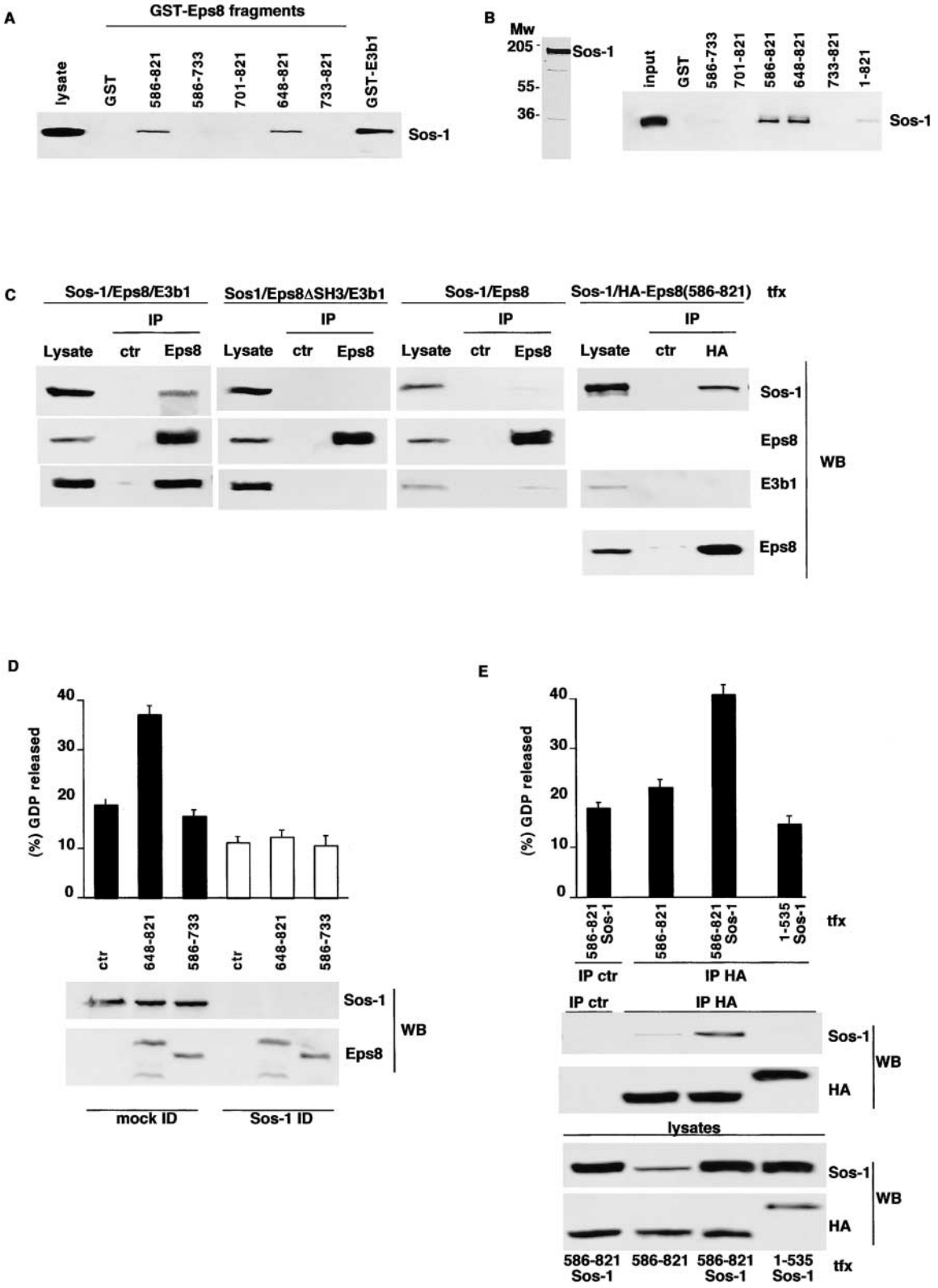

shown). The lanes "lysate" were loaded with 50 μg of total cellular lysates. (D) Top, Rac-specific GEF activity was measured in lysates of cells expressing the indicated Eps8 fragments (indicated underneath the bar graph. Ctr, control vector). Lysates were immunodepleted with an irrelevant (mock ID, solid bars) or by an anti–Sos-1 (Sos-1 ID, empty bars) antibody. The same immunodepleted lysates used for the GEF assays were analyzed by immunoblotting (WB, bottom) with the indicated antibodies. No Cdc42-specific GEF activity could be detected in the same lysates (not shown). (E) Top, Rac-specific GEF activity was measured in immunoprecipitates performed with anti-HA (IP HA) or an irrelevant antibody (IP ctr) on lysates of 293T cells transfected with the indicated expression vectors (tfx; the Eps8-based constructs were HA tagged). Bottom, aliquots of the immunoprecipitates (IP) used in the GEF assay, or total cellular lysates (50 μg) transfected with the expression vectors indicated at the bottom (tfx), were immunoblotted (WB) with the indicated antibodies.

Published August 27, 2001

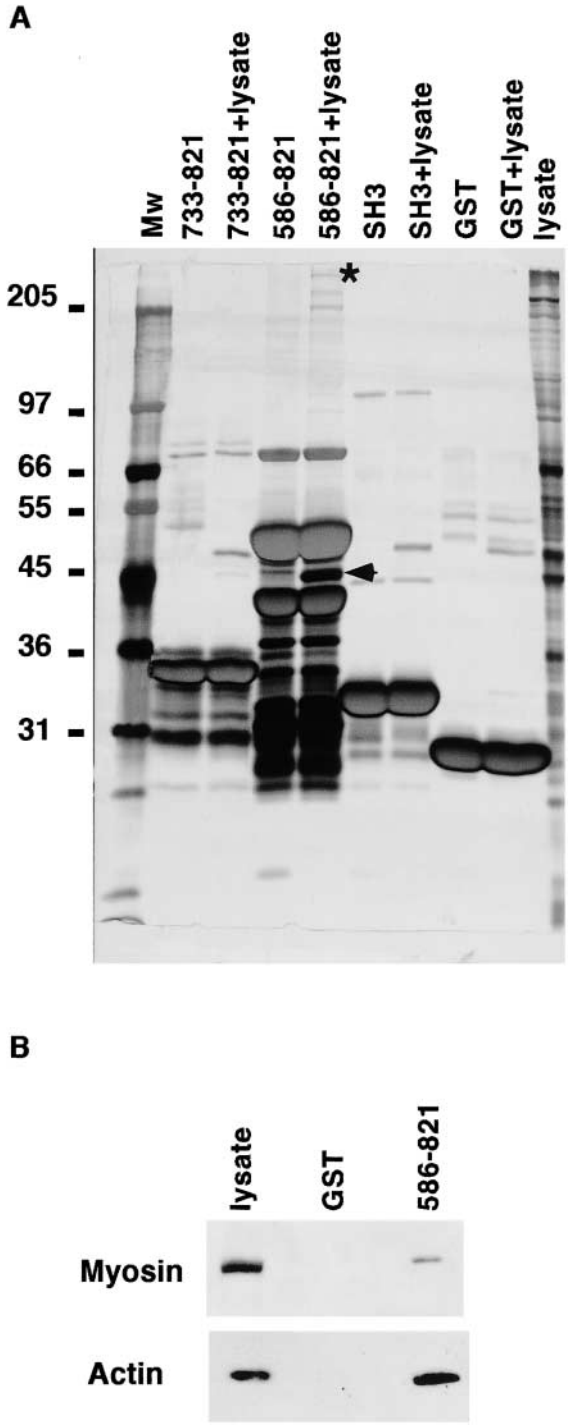

Figure 8. **Identification by MALDI-MS of novel interactors of the effector domain of Eps8.** (A) Various immobilized GST fusion fragments of the COOH-terminal region of Eps8 (amino acid boundaries are indicated on the top), GST-SH3 domain of Eps8 (SH3), or GST alone were incubated in the presence of lysis buffer as a control or with total cellular lysates (+lysates lanes) from mouse embryo fibroblasts. Specifically bound proteins were eluted in sample buffer and resolved by SDS-PAGE, followed by detection by silver staining. The marked (asterisk and arrowhead) bands were unequivocally identified by MALDI-MS, as described in Materials and methods, as the myosin II heavy chain and actin, respectively. Molecular weight markers are indicated in kD. (B) Total cellular lysates (1 mg) from mouse embryo fibroblasts were incubated with 5 μg of GST or GST-Eps8 (586–821). Detection was with antimyosin II heavy chain and antiactin antibodies as shown. The lane "lysate" was loaded with 100 μg of total cellular lysate.

ments. The minimal region capable of interacting with Sos-1 extended from amino acids 648 to 821, thus coinciding with the region required for the biological activity of the effector domain (Fig. 7, A and B). The interaction was likely direct, since GST-Eps8 (648–821) was able to bind, albeit with low stoichiometry, to native, eukaryotically produced, and purified (>90% purity) Sos-1 (Fig. 6 C). However, it cannot be formally excluded that copurified proteins tightly associated to Sos-1 might be responsible for the observed interaction.

As shown in Fig. 7 B, the effector region of Eps8, when alone, bound to purified Sos-1 at least 10-fold better than full length GST-Eps8. The marginal binding of full length GST-Eps8 might reflect the true ability of the holoprotein to interact with Sos-1 or an artifactual situation. Under this latter scenario, one could postulate that in vivo Eps8 does not bind to Sos-1 unless determinants in its COOH terminus are unmasked: a setting mimicked by the enucleation of the effector region from the holoprotein, or by partial unfolding of the bacterially expressed Eps8 full length molecule. To gain insight into this issue we studied the association in vivo of Sos-1 with either the effector region of Eps8 or with the holoprotein. Native Sos-1 could be efficiently recovered in HA-tagged Eps8 (586–821) immunoprecipitates of cells double transfected with Sos-1 and HA-Eps8 (586–821) (Fig. 7 C). No E3b1 could be detected in the same immunoprecipitates, even under conditions of E3b1 overexpression (not shown). On the contrary, the in vivo association between Sos-1 and Eps8 was strictly E3b1-dependent. Indeed, native Sos-1 could be readily recovered in Eps8 immunoprecipitates from triple Sos-1–E3b1–Eps8 transfectants, but not when an Eps8 mutant, unable to bind E3b1 due to a deletion in its SH3 domain (Eps8ΔSH3), was used (Sos-1–Eps8ΔSH3–E3b1 transfectants), or when E3b1 was not transfected along with Sos-1 and Eps8 (Sos-1–Eps8) (Scita et al., 1999; Fig. 7 C).

We then tested whether the biological and biochemical activity of the Eps8 effector region could activate Sos-1 Rac–specific GEF in vivo. First, a Rac-GEF assay was performed using lysates of cells expressing the effector domain of Eps8 or a ruffling-incompetent Eps8 fragment (586–733) which cannot bind to Sos-1. Expression of the effector region, but not of the ruffling-incompetent fragment, induced a substantial increase in Rac-specific GEF activity in vivo over the basal control values (Fig. 7 D). This effect was dependent on the presence of Sos-1 (or of another GEF, tightly associated to Sos-1), since no Rac-GEF activity could be detected in the same lysates upon immunodepletion of Sos-1 (Fig. 7 D). Second, we used in vitro assays that can score GEF activities in immunoprecipitates. Cells were transfected either with a construct containing the effector region, Eps8 (586–821), or with a control construct, Eps8 (1–535), alone or in combination with Sos-1. Rac-GEF activity could be readily detected when the Eps8 (586–821) protein was immunoprecipitated from cells coexpressing Eps8 (586–821) and Sos-1 (Fig. 7 E). Under these conditions, coimmunoprecipitation between Eps8 (586–821) and Sos-1 was detected (Fig. 7 E, bottom). Thus, the Eps8 effector region participates in the regulation of a Rac-specific GEF activity, which depends on the presence of Sos-1 or Sos-1–associated GEFs.

Published August 27, 2001

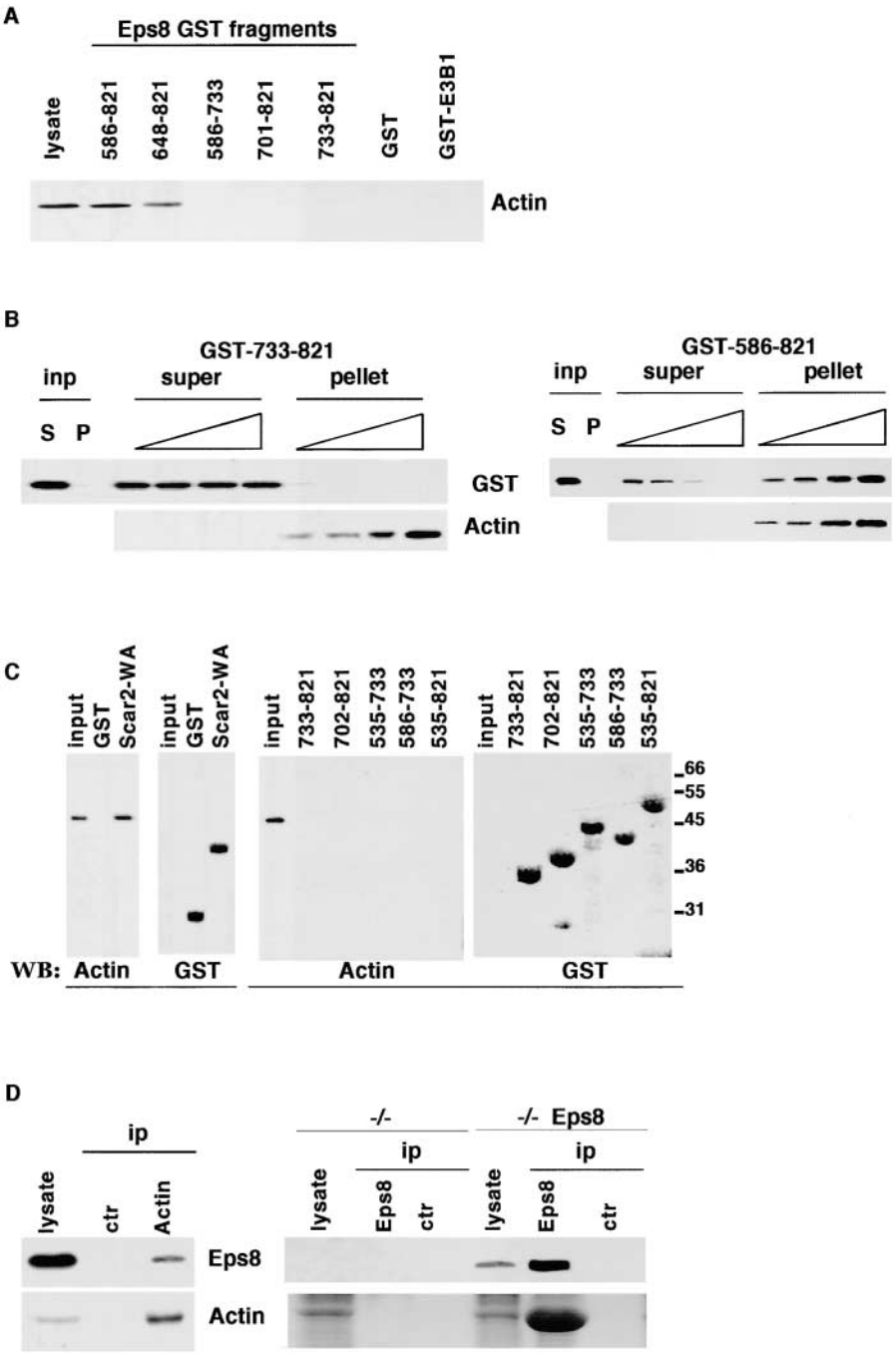

Figure 9. **Biochemical characterization of the interaction between the Eps8 and actin.** (A) Total cellular lysates from mouse embryo fibroblasts were incubated with 5 μg of each Eps8 fragment (all engineered as GST fusions; amino acid boundaries are indicated on the top) or GST or GST-E3b1, used as negative controls. Detection was with antiactin antibodies. The lane "lysate" was loaded with 50 μg of total cellular lysate. (B) Actin cosedimentation assay. The indicated fragments of Eps8 (left, Eps8 [733–821]; right, Eps8 [586–821]) fused to GST (2 μg) were mixed with increasing amounts of F-actin (0.5, 1.0, 2.0, and 10 μg, respectively), as described in Materials and methods, and the samples were ultracentrifuged. The input lanes (inp) show the supernatant (S) and the pellet (P) of a control tube, in which the GST fusion proteins were subjected to ultracentrifugation in the absence of F-actin. Detection was with anti-GST (top) or antiactin (bottom). (C) Purified, globular, nonmuscle actin (2 μg) was incubated with 5 μg of Sepharose-conjugated GST as a negative control, or GST-Scar-2-WA-domain (Scar2-WA) as a positive control (left; Miki et al., 1998), or GST-Eps8 fragments (amino acid boundaries are indicated in the top right panels). Bound proteins were recovered by low speed centrifugation and analyzed by immunoblotting (WB) with antiactin (Actin) and anti-GST (GST) antibodies. The lane "input" was loaded with 100 ng of G-actin. Molecular weight markers are indicated in kD. (D) Left, total cellular lysates from mouse embryo fibroblasts were immunoprecipitated with antiactin (Actin) or an irrelevant (ctr) antibody, followed by detection with the anti-Eps8 (top) or antiactin (bottom) antibodies. Right, total cellular lysates from Eps8 null mouse embryo fibroblasts (−/−), or from the same cells in which Eps8 was stably reintroduced (−/− Eps8), were immunoprecipitated with anti-Eps8 (Eps8) or the preimmune (ctr) sera, followed by detection with the anti-Eps8 (top) or antiactin (bottom) antibodies.

Eps8 interaction with F-actin, through its effector domain, directs its localization to site of actin remodeling

The effector domain of Eps8 was also responsible for its localization within F-actin–containing structures (Fig. 2 A). Thus, we looked for interactors with the Eps8 effector region. We used various GST-fused fragments of Eps8 in order to specifically recover proteins from cell lysates. As shown in Fig. 8 A, several cellular proteins were detected by silver staining. We concentrated our attention on those bands that were recovered by the 586–821 fragment (which is biologically active and properly localized), but not by the 733–821 or by the SH3 fragments (which are biologically inactive and delocalized), and subjected them to MALDI mass spectrometry and NanoElectrospray. Two proteins were unequivocally identified: actin and the myosin II heavy chain (Fig. 8 A). Both associations were confirmed by in vitro binding experiments (Fig. 8 B). Of note, the low stoichiometry of interaction between Eps8 and myosin II heavy chain suggested an indirect interaction, possibly mediated by actin. Therefore, we characterized the Eps8/actin association.

We mapped the minimal interaction surface of Eps8 with actin to a stretch of amino acids extending from position 648 to 821 (Fig. 9 A). Notably, this actin binding domain coincided with the minimal region required to elicit ruffling, bind to Sos-1, and colocalize with F-actin. Attempts to define determinants within this region individually responsible

Published August 27, 2001

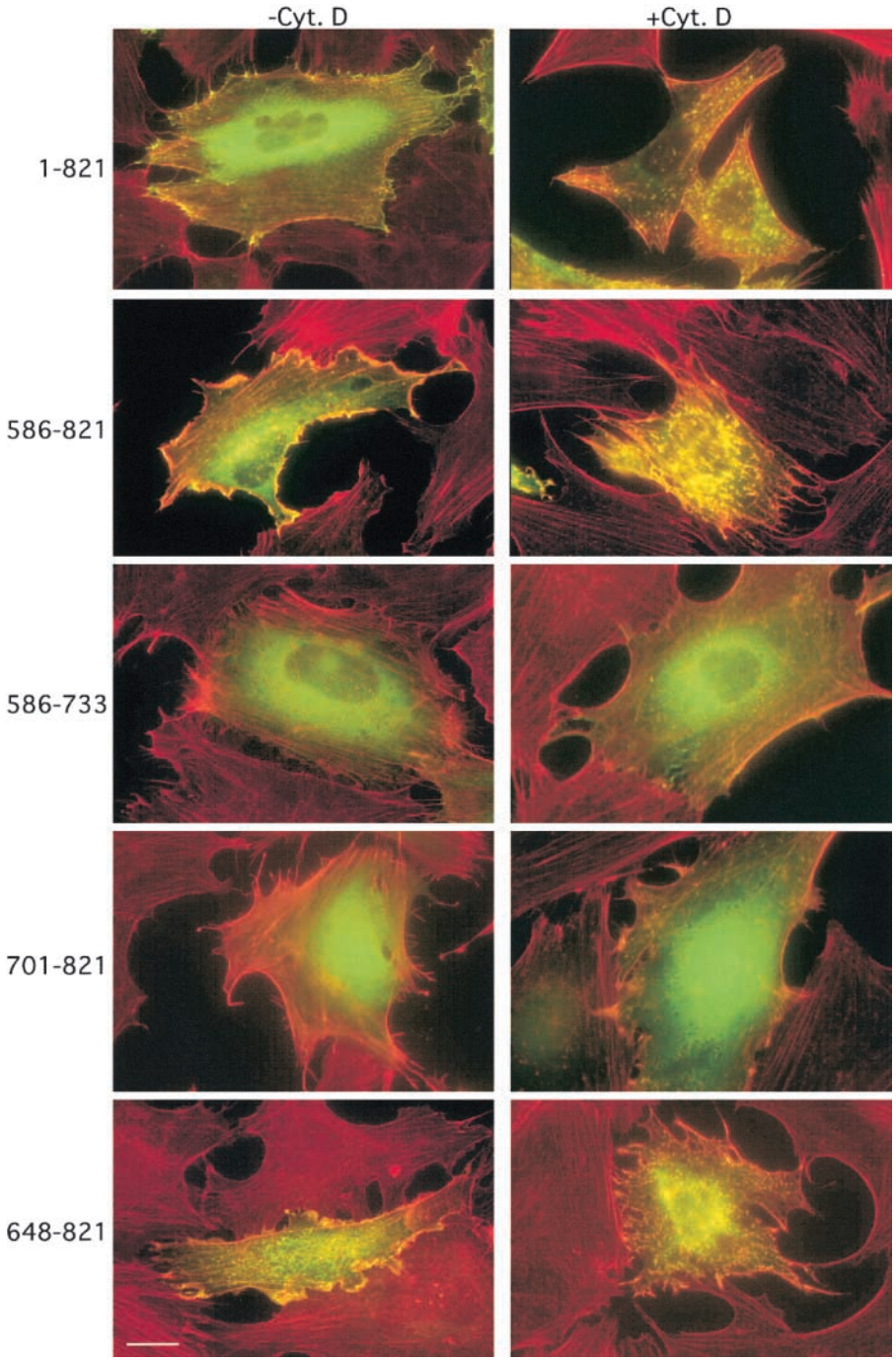

Figure 10. **Disruption of the actin filament meshwork by cytochalasin D leads to mislocalization of Eps8 and of the Eps8 effector domain.** Quiescent mouse embryo fibroblasts, transfected with the vectors encoding various GFP-tagged Eps8 fragments (amino acids boundaries are indicated on the left), were treated with cythocalasin D (100 nM) for 60 min (+Cyt. D) or with vehicle as a control (−Cyt. D). Cells were fixed and GFP was detected by epifluorescence (green). F-actin was evidenced by phalloidin staining (red). Note the colocalization of the Eps8 full length (1–821) and of the Eps8 fragments containing the effector domain (amino acids 648–821) with F-actin aggregates induced by treatment with cythocalasin D (yellow). Bar, 10 μM.

for binding to actin or to Sos-1 failed, suggesting that the integrity of the whole domain is required for both functions.

Actin exists in a monomeric globular (G-actin) or in a polymeric F-actin form. Therefore, GST fusion fragments of Eps8 were tested for in vitro binding to purified F-actin and G-actin in a high speed cosedimentation and in a low speed centrifugation assay, respectively (Matsudaira, 1992). A significant amount of GST-Eps8 (586–821) cosedimented with F-actin in a concentration-dependent manner, whereas control GST (not shown) or GST-Eps8 (586–733) (Fig. 9 B) were unable to do so. Furthermore, no binding to monomeric G-actin could be detected with any of the tested fusion proteins (Fig. 9 C, right). Notably, under the same conditions, efficient association between G-actin and the COOH-terminal region of Scar2, a known G-actin binding surface (Miki et al., 1998), could be observed (Fig. 9 C). Thus, the effector region of Eps8 binds directly to F-actin. However, no actin-polymerizing activity of the purified Eps8 effector region could be detected using a pyrene-conjugated actin polymerization assay (Karlsson, R., and G. Scita, personal communication). Thus, Eps8 might bind to F-actin in a manner similar to proteins like S-nexilin (Ohtsuka et al., 1998) or 1-afadin (Mandai et al., 1997), which are devoid of actin-bundling properties in vitro and serve as linkers between the actin cytoskeleton and subdomains on the plasma membrane.

Finally, we investigated whether the Eps8–F-actin association occurs in vivo. Native actin could be specifically coimmunopre-

Published August 27, 2001

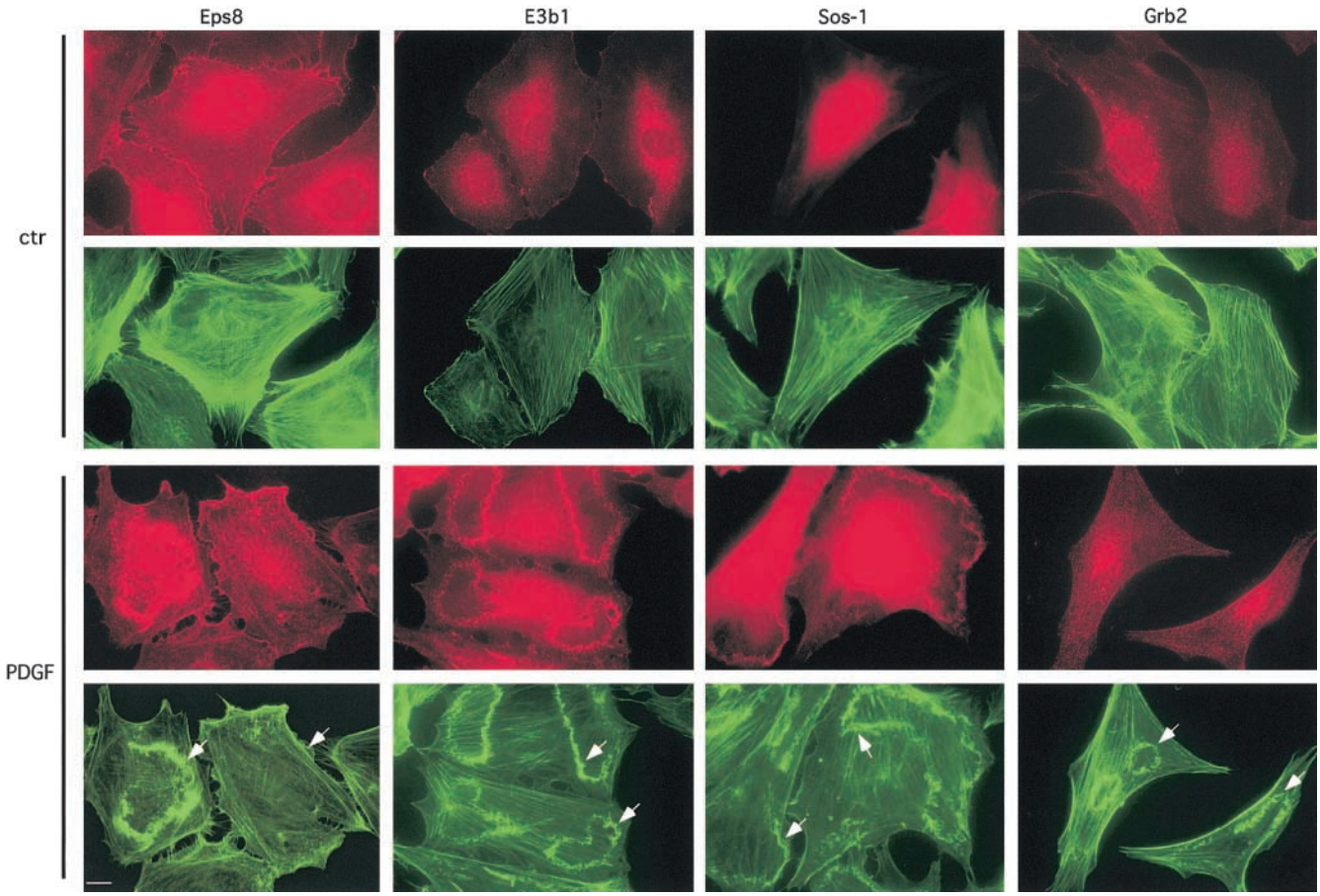

Figure 11. **Eps8, E3b1, and Sos-1, but not Grb2, accumulate in PDGF-induced membrane ruffles.** Serum-starved mouse embryo fibroblasts (ctr) were treated with 10 ng/ml of PDGF for 5 min (PDGF). Cells were then fixed and stained with antibodies indicated at the top (red), and with FITC-conjugated phalloidin to detect F-actin (green). Detection of Sos-1 was performed on cells which were transiently transfected with an expression vector coding Sos-1. Arrows point to ruffles. Bar, 10 mm.

cipitated with Eps8, whereas no association could be observed when preimmune sera were used, or in Eps8 immunoprecipitates performed on lysates from Eps8 null cells (Fig. 9 D).

The interaction in vivo between Eps8 and F-actin may dictate the proper intracellular localization of Eps8. In this case, disruption of the actin filaments should lead to Eps8 mislocalization. Treatment of cells with cytochalasin D, an inhibitor of actin polymerization (Goddette and Frieden, 1986; Sampath and Pollard, 1991), caused the disruption of the F-actin meshwork (Fig. 10). This resulted in the disruption of membrane ruffles and the scattered accumulation of short bundles of F-actin aggregates, which colocalized (Fig. 10) with Eps8 or with those Eps8 fragments containing an intact actin binding domain (Fig. 10). Thus, the integrity of the F-actin meshwork is required to direct Eps8 to its proper subcellular localization.

The localization of Eps8 and of the Eps8 effector domain to a site of actin polymerization suggests the possibility that, under physiological conditions, the trimeric complex Eps8–E3b1–Sos-1 is recruited to specific sites to elicit actin remodelling. Thus, we determined the intracellular localization of Sos-1 and of the adaptor molecules involved in the formation of Sos-1–based complexes after growth factor stimulation. Eps8, E3b1, and Sos-1, but not Grb2, rapidly relocalized and accumulated in membrane ruffles upon PDGFR activation (Fig. 11), pointing to an additional mechanism through which the activity of the tricomplex is regulated in vivo.

Discussion

We have shown previously that Eps8 is indispensable for the activation of the small GTPase Rac (Scita et al., 1999). This was mirrored by the detection in vivo of a tricomplex Eps8–E3b1–Sos-1, which was shown to display Rac-GEF activity in vitro (Scita et al., 1999). In this study, we provide evidence regarding the molecular mechanisms through which Eps8 affects the substrate specificity of Sos-1 and facilitates targeting of a Rac-activating complex to its proper subcellular sites. We identified a COOH-terminal region that is alone sufficient for both the actin-remodeling function and the localization to F-actin–containing structures of Eps8. We called this region the "effector region" of Eps8.

Several lines of evidence indicate that the effector region of Eps8 functions as a constitutively active variant of Eps8. First, genetic data demonstrated that the mechanism whereby the Eps8 effector region induces ruffles requires the activation and proper localization of Rac. Moreover, the effector region of Eps8 did not require Ras/PI3-K or Cdc42 to induce actin remodeling. This is in agreement with our pre-

Published August 27, 2001

vious work, which epistatically positioned Eps8 between Ras/PI3-K and Rac (Scita et al., 1999). Biochemical evidence also supported a role of the Eps8 effector region in the activation of Rac. Its transient expression led to activation in vivo of Rac and PAK65. Moreover, the overexpression of the effector region of Eps8 increased the levels of Rac-specific GEF activities in the cell by a mechanism which was shown to be directly dependent on the presence of Sos-1 (or of Sos-1–associated GEFs) and on the interaction between Sos-1 and the Eps8 effector region.

Thus, the effector region of Eps8 appears to signal in a manner indistinguishable from full length Eps8, albeit in a growth factor–independent fashion. Indeed, we showed that the overexpression of the effector region, but not of the full length Eps8 protein, is sufficient to elicit actin cytoskeleton remodeling. Thus, within the context of the full length Eps8 protein, a tight regulation of the effector function must be at play and determinants contained in the NH_2-terminal half of Eps8 are predicted to exert an inhibitory role. This mode of action is remarkably reminiscent of that of Wasp and its homologue N-Wasp, which link multiple signaling pathways to actin assembly. N-Wasp interacts with the Arp2/3 complex and activates the ability of the latter to nucleate actin filaments (for review see Mullins, 2000). A COOH-terminal domain of N-Wasp, the VCA domain, is sufficient when enucleated from the full length molecule to bind to the Arp2/3 complex and activate it (Mullins, 2000). Physiologically, however, activation of N-Wasp occurs when the molecule is stimulated by the proper set of upstream signals, including active Cdc42 and PIP2. These molecules bind cooperatively to N-Wasp and force it to adopt an open conformation, which exposes the VCA domain, allowing its effector function (Rohatgi et al., 1999; Higgs and Pollard, 2000; Prehoda et al., 2000).

In analogy to Wasp and N-Wasp, and based on our results, a model can therefore be proposed in which Eps8 that is normally inactive in the cell is activated by upstream signals and therefore rendered competent for activation of Rac. From our data, it appears that the key step in this series of events is the binding of the effector region of Eps8 to Sos-1. Indeed several activities, including Sos-1 binding, induction of Rac-specific GEFs and activation of Rac and Rac-dependent pathways, all cosegregated with the same fragment of Eps8. Thus, it is tempting to speculate that a latent, Rac-specific, GEF activity of Sos-1 is unmasked upon direct binding to the effector region of Eps8. In this scenario, the "activation" of Eps8 might correspond to a conformational change (or functionally equivalent mechanism), which renders its effector region available for direct interaction with Sos-1. A corollary of such a model is that full length Eps8 should not be able to bind to Sos-1 directly. Indeed, we show in this and previous studies (Scita et al., 1999) that association of Eps8 with Sos-1 is strictly dependent on the presence of the scaffolding molecule E3b1 (Fig. 7C). On the contrary, this latter molecule is not required for the interaction between the effector region of Eps8 and Sos-1 (Fig. 7, A–C), which are readily coimmunoprecipitated in vivo. To validate this model, we are presently attempting to reconstitute in vitro a Rac-specific GEF complex by using purified E3b1–Sos-1–Eps8 or purified Sos-1–Eps8 effector region.

Our model also provide clues as to how the Sos-1 Rac–specific GEF activity is regulated under physiological conditions, within the context of a trimeric complex where E3b1 scaffolds together Eps8 and Sos-1. We note that the affinity of Sos-1 for the effector region of Eps8 is rather low. Thus, the scaffolding function of E3b1 might provide an efficient mechanism of increasing the local concentration of the two binders (Eps8 and Sos-1) for the purpose of achieving a stoichiometry of interaction sufficient for biological output. Under conditions of overexpression of the effector region (but not of full length Eps8, according to our model), this requirement might be bypassed simply by virtue of mass action. Of course, this model does not exclude that other events, in addition to the simple Eps8–Sos-1 interaction, are required in vivo to activate the Rac-specific GEF function of Sos-1. One obvious level of regulation is the one exerted by growth factor stimulation, which might, among other effects, relieve the inhibition of Eps8. This could be achieved by a variety of mechanisms, including tyrosine phosphorylation of Eps8 or binding of phosphoinositides to the DH-PH domain of Sos-1 or to the PTB domain of Eps8. We are presently investigating these possibilities.

An additional level of regulation is highlighted by our findings of a physical direct interaction between Eps8 and F-actin, which mirrored the in vivo colocalization of Eps8 with F-actin–containing structures. This function is also contained within the effector region of Eps8. We could not identify determinants within this region that would allow the dissection of the abilities to bind to F-actin or to Sos-1. This might be due to a high degree of overlap between the two surfaces. In this case, single amino acid mutations might be required to identify the residues responsible for each individual interaction. The effector region of Eps8 did not appear to be endowed with intrinsic actin-polymerizing activity. Thus, the most likely functional role of the Eps8–F-actin interaction is that of directing Eps8 to sites where actin remodeling has to occur in response to extracellular stimuli. E3b1 and Sos-1 are also localized to F-actin–containing structures after growth factor stimulation of intact cells, and therefore interaction of Eps8 with F-actin might dictate the relocalization of the Rac-activating trimeric complex Eps8–E3b1–Sos-1 to sites where its activity is required.

Materials and methods

Expression vectors and antibodies

All eukaryotic expression vectors were generated in cytomegalovirus promoter–based constructs (pCDNA3, pCR3; In VitroGene). Vectors encoding for GFP fusion proteins were engineered in the pEGFP C1 plasmid (CLONTECH Laboratories, Inc.) by cloning the appropriate fragments, obtained by recombinant PCR, in frame with the GFP moiety. Where indicated, epitope tagging (either myc or HA) was obtained by recombinant PCR. Bacterial expression vectors were engineered to encode GST-fused and histidine-tagged proteins by cloning the appropriate fragments, obtained by recombinant PCR, in frame with GST or poly-His, respectively. All constructs were sequence verified. Details are available upon request. pMT2-HA-Sos-1 was a gift of D. Bar-Sagi (State University of New York at Stony Brook, Stony Brook, NY). Arf6T27N was provided by P. Chavrier (Chavrier P Institut Curie, Paris, France).

Antibodies (Ab) were: polyclonal anti-Eps8 (Fazioli et al., 1993), anti-E3b1 (Biesova et al., 1997), and anti-EGFR (Di Fiore et al., 1990) sera; rabbit polyclonals anti–Sos-1, anti-Grb2, and anti–ERK-1, (Santa Cruz Biotechnology, Inc.); monoclonals anti-myc and anti–v-H-Ras (Oncogene Research Products). Monoclonals antihistidine, antiactin, antimyosin II

heavy chain, and the chemicals, dimethyl pimelidate dihydrochloride, cytochalasin D, and wortmannin were from Sigma-Aldrich. Purified muscle actin was purchased from Cytoskeleton.

Transfection procedures and indirect immunofluorescence

Fibroblasts, seeded on gelatin, were transfected with the indicated expression vectors using the LIPOfectamine reagent (GIBCO BRL), according to the manufacturer's instructions. Alternatively, nuclei of quiescent fibroblasts were injected with 100 ng/ml of the appropriate expression vectors. 3–6 h later, cells were processed for immunostaining. At least 100 microinjected cells were analyzed in each experiment for indirect immunofluorescence. Cells were fixed in 4% paraformaldheyde for 10 min, permeabilized in 0.1% Triton X-100 and 2% BSA for 10 min, blocked with 2% BSA for 30 min, and then incubated with primary and secondary antibodies for 45 and 30 min, respectively. Transfected and/or microinjected cells were detected by staining of the protein encoded by the transfected or microinjected cDNA. F-actin was detected by staining with rhodamine-conjugated phalloidin (Sigma-Aldrich), used at a concentration of 6.7 U/ml (~0.22 μM). Alexa red and green secondary antibodies (Molecular Probes) were used. Where indicated, cells were treated with PDGF (10 ng/ml) or serum (10%) for 10 min before fixation.

Biochemical and functional assays

Standard procedures of protein analysis (in vitro binding assays, immunoprecipitations, and coimmunoprecipitations) were performed as described (Fazioli et al., 1993). The activities of MAPK, JNK, PAK65, and the levels of RacGTP were also measured as described (Scita et al., 1999). Whenever indicated, treatment was performed with EGF (100 ng/ml) after serum starvation for the indicated lengths of time.

Assays for Rac-GEF activity were performed as described (Scita et al., 1999). Data are the mean ± SE of at least three independent experiments performed in triplicate. Results are expressed as the [^{3}H]GDP released after 20 min relative to time 0 after subtracting the background counts released in control reactions (obtained by incubating [^{3}H]GDP-loaded Rac in exchange buffer).

For protein identification by MALDI-MS analysis, total cellular proteins were incubated in the presence of various immobilized GST fusion proteins. Specifically bound proteins were subjected to SDS-PAGE followed by detection with silver staining. The protein bands of interest were excised from one-dimensional polyacrylamide gels. After reduction and alkylation, proteins were digested "in gel" for 6 h at 37°C with sequencing-grade trypsin (Boehringer). Samples for MALDI analysis were prepared by using the "fast evaporation" method (Mann and Talbo, 1996). Mass spectra were recorded on a Voyager-DE STR BioSpectrometry workstation (PerSeptive Biosystems). Matrix-related ions and trypsin autolysis products were used for internal calibration. The peptide mass accuracy was >30 ppm (on average). The ProFound-Peptide Mapping software (Rockefeller University edition, v4.10.5) was used to search a nonredundant protein sequence database (searchable at the National Center for Biotechnology Information) with a list of peptide masses. The samples for MS/MS analysis were loaded onto a Poros R2 (PerSeptive Biosystems) microcolumm, desalted, and eluted into nanoelectrospray needles (Protana). Nanoelectrospray MS/MS analysis was performed on a quadrupole time-of-fight mass spectrometer (QSTAR; PerkinElmer). The resulting "peptide sequence tags" were used to search the nonredundant protein sequence database.

For cosedimentation assays with F-actin, monomeric human nonmuscle G-actin (1 mg/ml) was induced to polymerize into F-actin at 37°C for 60 min in F-buffer (5 mM Tris/HCl, pH 7.8, 1 mM ATP, 0.5 mM DTT, 0.2 mM $CaCl_2$, 0.2 mM $MgCl_2$, and 100 mM KCl) (Van Etten et al., 1994). Recombinant, purified GST fusion proteins (2 μM) were subsequently incubated with increasing concentration of F-actin in F-buffer for 45 min at 37°C. The mixtures were centrifuged in a TLA-100 rotor for 60 min at 100,000 *g*. Equal amounts of starting material, supernatants, and pellets were solubilized in loading buffer, boiled, and subjected to SDS-PAGE. Proteins were detected by immunoblotting using anti-GST and antiactin antibodies. The rate and the extent of actin polymerization in the presence of the Eps8 effector region was determined from the increase in fluorescence of pyrene actin that occurs when pyrene-labeled actin polymerizes, as described (Van Etten et al., 1994).

For Sos-1 purification, total cellular lysates from 293T cells, transfected with HA epitope–tagged Sos-1, were immunopurified onto an affinity column obtained by cross-linking anti-HA antibodies to immobilized protein G with dimethyl pimelidate dihydrochloride. After binding, the column was washed with the 10-bed volumes of lysis buffer containing 0.2% SDS. Bound Sos-1 was eluted with the peptide MYDVPDYAS, corresponding to the HA epitope tag. Sos-1 was >90% pure, as assessed by calculating the percentage of Sos-1 with respect to the total amount of protein. This was determined by subjecting serial dilutions of the purified material to SDS-PAGE followed by staining with Coomassie brilliant blue and compared with a standard curve of BSA. Similar results were obtained by comparing the intensity of the band corresponding to Sos-1 with the bands corresponding to contaminants and/or to Sos-1 degradation products.

Online supplemental material

Video 1 and Figure S1. Quiescent mouse embryo fibroblasts, microinjected with expression vectors for GFP-Eps8 (648-821) were kept at 37°C in a CO_2 incubator mounted on an inverted microscope (Olympus). Images were captured every 15 min with a coded CCD camera (Hamamatsu; speed, 6 frames/s at 15 min intervals). GFP epifluorescence was detected with a FITC filter set (Chromo Technology). The large fluorescent "blob" (visible in the top half in the final frames) probably represents a GFP-Eps8 (648–821)–transfected cell undergoing apoptosis after a round of cell division. A set of six consecutive images captured at the indicated time is also shown. The video and figure are available at http://www.jcb.org/content/vol154/issue5.

We thank D. Bar-Sagi, P. Chavrier, and Adriana Zucconi for reagents; and C. Matteucci for technical assistance. The microinjector Axiovert 100 (ZEISS) was donated by the Lattanzio family.

This work was supported by grants from Associazione Italiana Ricerca sul Cancro, the Armenise-Harward Foundation, and the Il Consiglio Nazionale delle Ricerche (CNR; Progetto Biotecnologie).

Submitted: 30 March 2001
Revised: 25 July 2001
Accepted: 26 July 2001

References

Bar-Sagi, D. 1994. The Sos (Son of Sevenless) protein. *Trends Endocrinol. Metab.* 5:164–169.

Bar-Sagi, D., and A. Hall. 2000. Ras and Rho GTPases: a family reunion. *Cell.* 103:227–238.

Biesova, Z., C. Piccoli, and W.T. Wong. 1997. Isolation and characterization of e3B1, an eps8 binding protein that regulates cell growth. *Oncogene.* 14:233–241.

Das, B., X. Shu, G.J. Day, J. Han, U.M. Krishna, J.R. Falck, and D. Broek. 2000. Control of intramolecular interactions between the pleckstrin homology and Dbl homology domains of Vav and Sos1 regulates Rac binding. *J. Biol. Chem.* 275:15074–15081.

Di Fiore, P.P., O. Segatto, F. Lonardo, F. Fazioli, J.H. Pierce, and S.A. Aaronson. 1990. The carboxy-terminal domains of erbB-2 and epidermal growth factor receptor exert different regulatory effects on intrinsic receptor tyrosine kinase function and transforming activity. *Mol. Cell. Biol.* 10:2749–2756.

Donaldson, J.G., and H. Radhakrishna. 2001. Expression and properties of ADP-ribosylation factor (ARF6) in endocytic pathways. *Methods Enzymol.* 329: 247–256.

Fan, P.D., and S.P. Goff. 2000. Abl interactor 1 binds to sos and inhibits epidermal growth factor- and v-abl-induced activation of extracellular signal-regulated kinases. *Mol. Cell. Biol.* 20:7591–7601.

Fazioli, F., L. Minichiello, V. Matoska, P. Castagnino, T. Miki, W.T. Wong, and P.P. Di Fiore. 1993. Eps8, a substrate for the epidermal growth factor receptor kinase, enhances EGF-dependent mitogenic signals. *EMBO J.* 12:3799–3808.

Goddette, D.W., and C. Frieden. 1986. Actin polymerization. The mechanism of action of cytochalasin D. *J. Biol. Chem.* 261:15974–15980.

Han, J., K. Luby-Phelps, B. Das, X. Shu, Y. Xia, R.D. Mosteller, U.M. Krishna, J.R. Falck, M.A. White, and D. Broek. 1998. Role of substrates and products of PI 3-kinase in regulating activation of Rac-related guanosine triphosphatases by Vav. *Science.* 279:558–560.

Higgs, H.N., and T.D. Pollard. 2000. Activation by Cdc42 and PIP(2) of Wiskott-Aldrich syndrome protein (WASp) stimulates actin nucleation by Arp2/3 complex. *J. Cell Biol.* 150:1311–1320.

Lim, L., E. Manser, T. Leung, and C. Hall. 1996. Regulation of phosphorylation pathways by p21 GTPases. The p21 Ras-related Rho subfamily and its role in phosphorylation signalling pathways. *Eur. J. Biochem.* 242:171–185.

Liu, B.P., and K. Burridge. 2000. Vav2 activates Rac1, Cdc42, and RhoA downstream from growth factor receptors but not beta1 integrins. *Mol. Cell. Biol.*

20:7160–7169.

Mandai, K., H. Nakanishi, A. Satoh, H. Obaishi, M. Wada, H. Nishioka, M. Itoh, A. Mizoguchi, T. Aoki, T. Fujimoto, Y. Matsuda, S. Tsukita, and Y. Takai. 1997. Afadin: a novel actin filament-binding protein with one PDZ domain localized at cadherin-based cell-to-cell adherens junction. *J. Cell Biol*. 139: 517–528.

Mann, M., and G. Talbo. 1996. Developments in matrix-assisted laser desorption/ionization peptide mass spectrometry. *Curr. Opin. Biotechnol*. 7:11–19.

Matsudaira, P. 1992. Mapping structural and functional domain in actin binding protein. *In* The Cytoskeleton: A Practical Approach. K.L. Carraway and C.A.C. Carraway, editors. Oxford University, London. 73–98.

Miki, H., S. Suetsugu, and T. Takenawa. 1998. WAVE, a novel WASP-family protein involved in actin reorganization induced by Rac. *EMBO J*. 17:6932–6941.

Mongiovi, A.M., P.R. Romano, S. Panni, M. Mendoza, W.T. Wong, A. Musacchio, G. Cesareni, and P.P. Di Fiore. 1999. A novel peptide-SH3 interaction. *EMBO J*. 18:5300–5309.

Moores, S.L., L.M. Selfors, J. Fredericks, T. Breit, K. Fujikawa, F.W. Alt, J.S. Brugge, and W. Swat. 2000. Vav family proteins couple to diverse cell surface receptors. *Mol. Cell. Biol*. 20:6364–6373.

Mullins, R.D. 2000. How WASP-family proteins and the Arp2/3 complex convert intracellular signals into cytoskeletal structures. *Curr. Opin. Cell Biol*. 12:91–96.

Nimnual, A.S., B.A. Yatsula, and D. Bar-Sagi. 1998. Coupling of Ras and Rac guanosine triphosphatases through the Ras exchanger Sos. *Science*. 279:560–563.

Ohtsuka, T., H. Nakanishi, W. Ikeda, A. Satoh, Y. Momose, H. Nishioka, and Y. Takai. 1998. Nexilin: a novel actin filament-binding protein localized at cell-matrix adherens junction. *J. Cell Biol*. 143:1227–1238.

Prehoda, K.E., J.A. Scott, R. Dyche Mullins, and W.A. Lim. 2000. Integration of multiple signals through cooperative regulation of the N-WASP-Arp2/3 complex. *Science*. 290:801–806.

Provenzano, C., R. Gallo, R. Carbone, P.P. Di Fiore, G. Falcone, L. Castellani, and S. Alema. 1998. Eps8, a tyrosine kinase substrate, is recruited to the cell cortex and dynamic F-actin upon cytoskeleton remodeling. *Exp. Cell Res*. 242:186–200.

Radhakrishna, H., O. Al-Awar, Z. Khachikian, and J.G. Donaldson. 1999. ARF6 requirement for Rac ruffling suggests a role for membrane trafficking in cortical actin rearrangements. *J. Cell Sci*. 112:855–866.

Rodriguez-Viciana, P., P.H. Warne, A. Khwaja, B.M. Marte, D. Pappin, P. Das, M.D. Waterfield, A. Ridley, and J. Downward. 1997. Role of phosphoinositide 3-OH kinase in cell transformation and control of the actin cytoskeleton by Ras. *Cell*. 89:457–467.

Rohatgi, R., L. Ma, H. Miki, M. Lopez, T. Kirchhausen, T. Takenawa, and M.W. Kirschner. 1999. The interaction between N-WASP and the Arp2/3 complex links Cdc42-dependent signals to actin assembly. *Cell*. 97:221–231.

Sampath, P., and T.D. Pollard. 1991. Effects of cytochalasin, phalloidin, and pH on the elongation of actin filaments. *Biochemistry*. 30:1973–1980.

Schlessinger, J. 2000. Cell signaling by receptor tyrosine kinases. *Cell*. 103:211–225.

Schuebel, K.E., N. Movilla, J.L. Rosa, and X.R. Bustelo. 1998. Phosphorylation-dependent and constitutive activation of Rho proteins by wild-type and oncogenic Vav-2. *EMBO J*. 17:6608–6621.

Scita, G., J. Nordstrom, R. Carbone, P. Tenca, G. Giardina, S. Gutkind, M. Bjarnegard, C. Betsholtz, and P.P. Di Fiore. 1999. EPS8 and E3B1 transduce signals from Ras to Rac. *Nature*. 401:290–293.

Scita, G., P. Tenca, E. Frittoli, A. Tocchetti, M. Innocenti, G. Giardina, and P.P. Di Fiore. 2000. Signaling from Ras to Rac and beyond: not just a matter of GEFs. *EMBO J*. 19:2393–2398.

Shi, Y., K. Alin, and S.P. Goff. 1995. Abl-interactor-1, a novel SH3 protein binding to the carboxy-terminal portion of the Abl protein, suppresses v-abl transforming activity. *Genes Dev*. 9:2583–2597.

Trenkle, T., M. McClelland, K. Adlkofer, and J. Welsh. 2000. Major transcript variants of VAV3, a new member of the VAV family of guanine nucleotide exchange factors. *Gene*. 245:139–149.

Van Etten, R.A., P.K. Jackson, D. Baltimore, M.C. Sanders, P.T. Matsudaira, and P.A. Janmey. 1994. The COOH terminus of the c-Abl tyrosine kinase contains distinct F- and G-actin binding domains with bundling activity. *J. Cell Biol*. 124:325–340.

Zhang, Q., J. Calafat, H. Janssen, and S. Greenberg. 1999. ARF6 is required for growth factor- and rac-mediated membrane ruffling in macrophages at a stage distal to rac membrane targeting. *Mol. Cell. Biol*. 19:8158–8168.